

FOKKER-PLANCK-BASED CONTROL OF A TWO-LEVEL OPEN QUANTUM SYSTEM

M. ANNUNZIATO

*Università degli Studi di Salerno,
Dipartimento di Matematica, Via Ponte Don Melillo,
84084 Fisciano, Italia
mannunzi@unisa.it*

A. BORZI*

*Institut für Mathematik, Universität Würzburg,
Emil-Fischer-Strasse 30,
97074 Würzburg, Germany
alfio.borzi@mathematik.uni-wuerzburg.de*

Received 4 June 2012

Revised 14 September 2012

Accepted 7 November 2012

Published 12 March 2013

Communicated by P. A. Markowich

The control of a two-level open quantum system subject to dissipation due to environment interaction is considered. The evolution of this system is governed by a Lindblad master equation which is augmented by a stochastic term to model the effect of time-continuous measurements. In order to control this stochastic master equation model, a Fokker-Planck control framework is investigated. Within this strategy, the control objectives are defined based on the probability density functions of the two-level stochastic process and the controls are computed as minimizers of these objectives subject to the constraints represented by the Fokker-Planck equation. This minimization problem is characterized by an optimality system including the Fokker-Planck equation and its adjoint. This optimality system is approximated by a second-order accurate, stable, conservative and positive-preserving discretization scheme. The implementation of the resulting open-loop controls is realized with a receding-horizon algorithm over a sequence of time windows. Results of numerical experiments demonstrate the effectiveness of the proposed approach.

Keywords: Fokker-Planck equation; stochastic process; optimal control theory; open quantum system; stochastic Schrödinger equation.

AMS Subject Classification: 35Q84, 49K20, 60G99, 65M06, 93E03, 81V80, 82C31

*Corresponding author

1. Introduction

The spectacular progress in the development of nano-systems where quantum states are used and manipulated for the encoding and processing of quantum information shows, on the one hand, the enormous technological potential of envisioned quantum devices and, on the other hand, the limitation of modeling these systems as closed quantum systems. In fact, sophisticated laboratory measurements demonstrate that any nano-device suffers an uncontrollable coupling with the environment; see, e.g. Ref. 20. Moreover, these devices are subject to measurements and any control mechanism also determines an exterior coupling. For this reason, the modeling of the environmental impact and of measurements is essential. This motivates the theory of open quantum systems describing the interaction of a quantum model with another one representing the environment, while the combined system is assumed to be closed. In this theory, the dynamical evolution of the open system is then described with an effective equation of motion called the master equation (ME). Furthermore, once the open system is subject to continuous measurements, an extension of the master equation that includes stochastic terms is required. These terms are seen as randomness originating from the measurement process; see Ref. 2.

We remark that in recent years, a large research effort has been put into the field of optimal control of closed quantum systems. We refer to Ref. 6 for a review and many references on the subject. In particular, we refer to, e.g. Refs. 5, 22 for computational methodologies for finite-dimensional quantum control problems and to Ref. 3 and references therein, for controllability issues. Concerning the control of open quantum systems, the literature is quite sparse; see, e.g. Refs. 4, 10 and 28. In this context, our work represents the first attempt to develop a mathematical control framework for open quantum systems subject to continuous measurements.

We are interested in the control of open quantum systems subject to measurements whose density operator is governed by a master equation that can be related to a stochastic Schrödinger equation (SSE) for the quantum state; see Ref. 32. That is, the ensemble of quantum states generated by the SSE reproduces the density operator modeled by the master equation. The advantages of the SSE approach are: (a) lower dimensionality of the problem, since the SSE provides the state described by an N -dimensional complex-valued function while the ME describes an $N \times N$ density matrix; and (b) easier interpretation and modeling of environmental and instrument interactions.

Our motivation for considering the control of open quantum systems is manifold and stems from the need to control states of quantum models through external fields. In fact, any conceivable device aims at manipulating quantum systems for a given purpose and this manipulation is possible using external fields. Moreover, efficient devices require optimal control fields with least energy that could also be used to counteract environmental losses. In any case, the design of these control fields should take into consideration the influence of the environment and must be

robust with respect to fluctuations due to device-environment interactions and to measurements. This is a very challenging open problem that is attracting great attention of mathematical and natural sciences communities. We notice that there is a general consensus about the modeling of open quantum systems that focuses on the formulation of the so-called Lindblad master equation. On the other hand, some models have been proposed to describe the effect of the measurement in continuous or discrete time. However, in these cases the idea to interpret the action of a measurement device as a source of stochasticity in the Schrödinger equation and correspondingly in the master equation appears very promising; see, e.g. Refs. 2, 25 and references therein. Therefore, within this framework it becomes important to define a control strategy for this type of stochastic master equations.

The purpose of this paper is to present an effective control strategy that, on the one hand, exploits the relationship between the stochastic Schrödinger equation and the stochastic Lindblad master equation, and on the other hand introduces the Fokker–Planck (FP) equation that models the evolution of the probability density function (PDF) of the stochastic processes. The use of the PDF allows us to consider deterministic objectives and the use of the FP equation makes possible to compute robust controls that take into account the statistics of the stochastic evolution.

This development involves notions from quantum mechanics and statistical physics, scientific computing and optimal control theory. We discuss this sophisticated framework in details considering a representative model of quantum mechanics, namely the two-level quantum system that plays a fundamental role in quantum optics and quantum computation and relates to classical Bloch systems that are central in nuclear magnetic resonance (NMR).

In the next section, we illustrate a representative two-level spin quantum system. We start from a closed system and discuss the case of a statistical ensemble of spins which is described by a density matrix governed by a Liouville–von Neumann master equation. Further, we introduce a dissipation term to obtain the Lindblad equation that we use to derive the equations of motion for the mean magnetic moment in Cartesian and in angular coordinates. Then, we formulate a special case of these equations including stochastic terms corresponding to the so-called heterodyne measurements.

In Sec. 3, we introduce the Fokker–Planck equation for the stochastic master equation of the two-level model. This is a partial differential equation of parabolic type defined in the space of angular coordinates of a sphere. Because the solution of the FP equation models the PDF of the stochastic process, we have the additional requirements of positiveness and conservativeness of the PDF. In Sec. 4, we formulate an optimal control problem for the PDF of the two-level stochastic process. We assume a control mechanism through magnetic fields as it is common in the closed version of quantum spin systems. To characterize the solution to the resulting control problem, we determine the optimality systems consisting in the FP equation, an adjoint FP equation marching backwards in time, and two optimality conditions. The derivation of the adjoint equation is not straightforward and we

report all details in the Appendix. The solution of the optimality system provides an optimal control vector that applies to the system during a short time window. This procedure of computing a new optimal control in each subsequent time window results in a model predictive control strategy that implements a closed loop control scheme. In Sec. 5, we discuss a special second-order accurate and stable discretization scheme that guarantees positivity and conservativeness of the PDF solution. We extend this scheme to the adjoint FP equation and show that the discrete adjoint FP equation results in the algebraic transpose of the discrete FP equation. In Sec. 6, we report results of numerical experiments to validate the ability of our optimal control strategy. We show that our FP control scheme is able to drive the PDF of the magnetic moment orientation. We consider the cases of an initial Gaussian distribution at the equator and a target distribution at the south pole and vice versa. We also use the controls computed with our closed-loop control mechanism directly in the stochastic model to demonstrate the effectiveness of the control on the single trajectories. A section of conclusion completes this work.

2. Two-Level Systems and the Bloch Sphere

In quantum mechanics, the space of pure states of a two-level system is a two-dimensional complex Hilbert space, which is a geometrical sphere (surface) with the antipodal points corresponding to mutually orthogonal state vectors, e.g. the spin-up and spin-down states of an electron. According to the usual physics notation, we denote these two states with $|0\rangle$ and $|1\rangle$, respectively. All other points on the sphere correspond to mixed states.

A two-level quantum state can be written as a complex superposition of the basis vectors $|0\rangle$ and $|1\rangle$. Thus any state $|\psi\rangle$ has the normalized representation (see, e.g. Ref. 2)

$$|\psi\rangle = \cos\left(\frac{\theta}{2}\right)|0\rangle + e^{i\varphi}\sin\left(\frac{\theta}{2}\right)|1\rangle,$$

where $0 \leq \theta \leq \pi$ and $0 \leq \varphi < 2\pi$ are the spherical coordinates on the Bloch sphere depicted in Fig. 1. These coordinates specify a point, the Bloch vector given as follows:

$$\mathbf{m} = (x, y, z) = (\sin(\theta)\cos(\varphi), \sin(\theta)\sin(\varphi), \cos(\theta)).$$

The Hamiltonian of a two-level spin system is given by

$$H = \frac{\hbar}{2}\omega\sigma_z - \frac{\hbar}{2}(\Omega^*(t)\sigma + \Omega(t)\sigma^\dagger), \quad (2.1)$$

where the operators $\boldsymbol{\sigma} = (\sigma_x, \sigma_y, \sigma_z)$ are the following Pauli matrices

$$\sigma_x = \begin{pmatrix} 0 & 1 \\ 1 & 0 \end{pmatrix}, \quad \sigma_y = \begin{pmatrix} 0 & -i \\ i & 0 \end{pmatrix}, \quad \sigma_z = \begin{pmatrix} 1 & 0 \\ 0 & -1 \end{pmatrix}$$

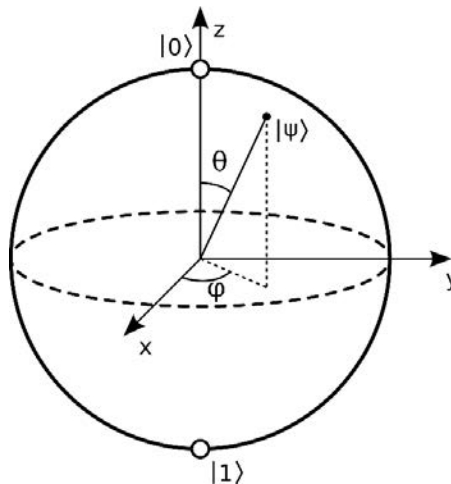


Fig. 1. The Bloch sphere.

and σ and σ^\dagger are the “lowering” and “raising” operators, respectively, defined as follows:

$$\sigma = (\sigma_x - i\sigma_y)/2, \quad \sigma^\dagger = (\sigma_x + i\sigma_y)/2.$$

The constant ω may represent a detuning field and the Rabi frequency $\Omega(t)$ is a complex function that is proportional to the slowly-varying complex amplitude of the control laser field (in case of, e.g. qubits) or of the RF-field (in NMR).

If we consider a closed two-level system as a statistical ensemble, then it can be described by its density matrix $\rho \in \mathbb{C}^{2 \times 2}$ given by

$$\rho = \frac{1}{2}(I + \mathbf{m} \cdot \boldsymbol{\sigma}),$$

where $I \in \mathbb{C}^{2 \times 2}$ is the identity.

The evolution of the two-level quantum states is governed by the Schrödinger equation with the Hamiltonian given by (2.1), that results in the following Liouville–von Neumann master equation for the density operator

$$i\hbar \frac{\partial \rho}{\partial t} = [H, \rho],$$

where the commutator $[A, B] = AB - BA$.

The density matrix of a quantum system serves to calculate the mean value of any operator of a physical observable associated to the system. In particular, the expectation value of the spin orientation is given by $\mathbf{m} = \langle \boldsymbol{\sigma} \rangle = \text{Tr}(\rho \boldsymbol{\sigma})$ (Tr means trace). Notice that the eigenvalues of ρ are given by $(1 \pm |\mathbf{m}|)/2 \geq 0$.

Using the Liouville–von Neumann master equation, we can compute the evolution of the magnetic moment of an ensemble of (closed) two-level spin systems. Consider the quantum magnetic moment operator given by $\boldsymbol{\mu} = \gamma \frac{1}{2} \hbar \boldsymbol{\sigma}$, where

γ is the gyromagnetic ratio. The Hamiltonian of μ in an external magnetic field $-\gamma\mathbf{B} = (\Omega_r, \Omega_i, \omega)$ is given by $\mathbf{H} = -\boldsymbol{\mu} \cdot \mathbf{B}$. Therefore we have

$$\frac{\partial \rho}{\partial t} = \frac{1}{2} \frac{\partial \mathbf{m}}{\partial t} \cdot \boldsymbol{\sigma} = i \frac{1}{4} \gamma [(\mathbf{B} \cdot \boldsymbol{\sigma})(\mathbf{m} \cdot \boldsymbol{\sigma}) - (\mathbf{m} \cdot \boldsymbol{\sigma})(\mathbf{B} \cdot \boldsymbol{\sigma})] = -\frac{1}{2} \gamma \mathbf{B} \times \mathbf{m} \cdot \boldsymbol{\sigma}.$$

(Use $[\sigma_a, \sigma_b] = 2i\epsilon_{abc}\sigma_c$.) Hence, we obtain the following Bloch equations

$$\frac{\partial \mathbf{m}}{\partial t} = -\gamma \mathbf{B} \times \mathbf{m}.$$

These equations are well known in NMR where they describe the evolution of magnetic spin in a “static” magnetic field B_z along the z -axis and a control field $(B_x(t), B_y(t))$ in the x, y -plane. We refer to Ref. 3 for a detailed study of the controllability of this Bloch system.

Closed quantum systems are assumed to be isolated from any interaction with the environment. In the case of a two-level system, a more realistic description is to consider an open system interacting with an external electromagnetic field.

In this case, the corresponding statistical ensemble is governed by the Liouville–von Neumann master equation augmented with an additional “dissipator” term $D(\rho)$ as follows:

$$i\hbar \frac{\partial \rho}{\partial t} = [H, \rho] + i\hbar D(\rho). \quad (2.2)$$

Specifically, in case of spin-electromagnetic interaction and using the dipole approximation, we have

$$D(\rho) = g\sigma\rho\sigma^\dagger - \frac{g}{2}\{\sigma^\dagger\sigma, \rho\}, \quad (2.3)$$

where $\{A, B\} = AB + BA$, and g is a phenomenological damping constant. In the presence of a thermal bath and of dephasing effects, additional terms enter in the construction of the dissipator; see, e.g. Ref. 2. For ease of notation, in the following we set $\hbar = 1$.

Equation (2.2) is the Lindblad master equation. In correspondence to the Hamiltonian (2.1) and (2.3), the Lindblad equation results in the following equation for the expectation values of the spin components, $\mathbf{m} = (x, y, z)$. We have

$$\begin{aligned} \dot{x} &= -\frac{g}{2}x - \omega y + \Omega_i z, \\ \dot{y} &= \omega x - \frac{g}{2}y + \Omega_r z, \\ \dot{z} &= -\Omega_i x - \Omega_r y - g(z + 1), \end{aligned}$$

where $\Omega = \Omega_r + i\Omega_i$ is the control field.

In terms of spherical coordinates, we obtain $\varphi = \arctan(y/x)$ and $\theta = \arccos(z)$ and the Bloch equations with $\Omega_i = -au$ and $\Omega_r = av$ become

$$\dot{\varphi} = A_\varphi(\varphi, \theta, u, v), \quad (2.4)$$

$$\dot{\theta} = A_\theta(\varphi, u, v) + g \frac{1 + \cos(\theta)}{\sin(\theta)}, \quad (2.5)$$

where

$$A_\varphi(\varphi, \theta, u, v) = \omega + a \cot(\theta)(u \sin(\varphi) + v \cos(\varphi)), \quad (2.6)$$

$$A_\theta(\varphi, u, v) = -a(u \cos(\varphi) - v \sin(\varphi)). \quad (2.7)$$

Equations (2.4)–(2.7) model the evolution of the orientation of mean magnetic moment of a two-level spin system with dissipation due to dipole interaction.

The next step in the modeling of open quantum systems is to develop a theory of measurements, that is, to model the action of a measurement operation on the system's dynamics. For this purpose, two types of stochastic Schrödinger equations^{9,11} are considered that correspond to measurements in continuous time and to measurements at different instants of time, respectively. The former case can be seen as a diffusion process, while the latter corresponds to a jumping process. In both cases, the result of the experiment and its effect on the dynamics of the system is considered as a random variable within the set of possible values. This framework also includes the case of detection of fluorescent light, where the measurement does not introduce extra perturbation on the dynamics; see, e.g. Ref. 2.

In the discussion above, we try to illustrate in general terms the modeling process starting from a two-level closed quantum system to an open one. Now, to continue our discussion, we focus on a specific model of physical interest. We discuss an open two-level system subject to heterodyne measurements (diffusive case) proposed in Ref. 32. This setting corresponds to the following stochastic Schrödinger equation (SSE); see also Ref. 11. We have

$$d\psi = -\left(iH + \frac{g}{2}\sigma^\dagger\sigma - g\langle\sigma^\dagger\rangle\sigma\right)\psi dt + \sqrt{g}\sigma\psi dW, \quad (2.8)$$

where dW represents a complex Wiener process.

As shown in Refs. 2 and 25, in correspondence to a SSE it is possible to formulate a stochastic master equation and vice versa. In particular, for the SSE given in (2.8), the following stochastic master equation in spherical coordinates is obtained

$$\begin{cases} d\varphi(t) = B_\varphi(\varphi, \theta, u, v)dt + \sigma_{11}(\varphi, \theta)dW_1 + \sigma_{12}(\varphi, \theta)dW_2, \\ d\theta(t) = B_\theta(\varphi, \theta, u, v)dt + \sigma_{21}(\varphi, \theta)dW_1 + \sigma_{22}(\varphi, \theta)dW_2, \end{cases} \quad (2.9)$$

where

$$B_\varphi(\varphi, \theta, u, v) = A_\varphi(\varphi, \theta, u, v),$$

$$B_\theta(\varphi, \theta, u, v) = A_\theta(\varphi, u, v) + g \frac{1 + \cos(\theta)}{\sin(\theta)} (1 - (1 + \cos(\theta)) \cos(\theta)/4),$$

$$\sigma_{11}(\varphi, \theta) = -\sqrt{\frac{g}{2}} \frac{1 + \cos(\theta)}{\sin(\theta)} \sin(\varphi), \quad \sigma_{12}(\varphi, \theta) = \sqrt{\frac{g}{2}} \frac{1 + \cos(\theta)}{\sin(\theta)} \cos(\varphi),$$

$$\sigma_{21}(\varphi, \theta) = \sqrt{\frac{g}{2}} (1 + \cos(\theta)) \cos(\varphi), \quad \sigma_{22}(\varphi, \theta) = \sqrt{\frac{g}{2}} (1 + \cos(\theta)) \sin(\varphi),$$

where $dW_1 = \sqrt{2} \operatorname{Re}(dW)$, $dW_2 = \sqrt{2} \operatorname{Im}(dW)$ and variance $E(dW_1^2) = E(dW_2^2) = dt$.

Notice that the differential model for an open two-level system given by (2.4)–(2.7) is similar to the deterministic part of (2.9) that includes a measurement model and a slightly different dissipator. Both equations describe the orientation of the mean magnetic moment, while it spreads during the evolution. It is clear that taking the statistical expectation of (2.9), one recovers the deterministic differential model, because the expectation of the Wiener processes dW_1 and dW_2 is zero.

We remark that with stochastic models a control strategy is required that provides controllers that are robust for all trajectories resulting from the stochastic perturbation.

3. The Fokker–Planck Equation for the Two-Level Model

A very important consequence of modeling an open quantum system subject to measurement as a stochastic differential model is that we can investigate this system from a statistical point of view and notice that the state of a stochastic process can be completely characterized by the shape of its statistical distribution that is represented by the probability density function (PDF). The next important consequence is that the evolution of the PDF associated to a stochastic process is modeled by a Fokker–Planck (FP) equation; see, e.g. Ref. 27.

Corresponding to the stochastic Bloch equation (2.9), we obtain the following FP equation, where we include the control terms. We have

$$\begin{aligned} \partial_t f = & -\partial_\varphi(A_\varphi(\varphi, \theta, u, v)f) \\ & -\partial_\theta \left[\left(A_\theta(\varphi, u, v) + g \frac{1 + \cos(\theta)}{\sin(\theta)} \left(1 - \frac{(1 + \cos(\theta)) \cos(\theta)}{4} \right) \right) f \right] \\ & + \frac{g}{4} \partial_\varphi^2 \left(\frac{1 + \cos(\theta)}{1 - \cos(\theta)} f \right) + \frac{g}{4} \partial_\theta^2 ((1 + \cos(\theta))^2 f), \end{aligned} \quad (3.1)$$

where $\varphi \in [0, 2\pi]$, $\theta \in (0, \pi)$ and the solution $f(\varphi, \theta, t) \geq 0$ is required to be non-negative and its integral on the domain be conserved and normalized as follows:

$$\int_0^{2\pi} \int_0^\pi f(\varphi, \theta, t) d\theta d\varphi = 1. \quad (3.2)$$

To complete the formulation of our FP problem, we have to specify the initial PDF denoted by $\rho(\varphi, \theta)$ at time t_0 . Clearly, ρ should be non-negative and normalized $\int_0^{2\pi} \int_0^\pi \rho(\varphi, \theta, t_0) d\theta d\varphi = 1$. Furthermore, we need to specify the following periodicity conditions

$$(\varphi, \theta + \Delta\theta) = \begin{cases} (\varphi + \pi, -\theta') & \text{if } \theta' = \theta + \Delta\theta \in (-\pi, 0), \\ (\varphi + \pi, 2\pi - \theta') & \text{if } \theta' = \theta + \Delta\theta \in (\pi, 2\pi), \end{cases} \quad (3.3)$$

$$(\varphi + \Delta\varphi, \theta) = (\varphi', \theta)\varphi' = \text{mod}(\varphi + \Delta\varphi, 2\pi). \quad (3.4)$$

Notice that our FP equation models the evolution of the PDF of the orientation of the spin in spherical coordinates. Therefore it is defined on the “flat” domain $S = (0, \pi) \times [0, 2\pi)$ and not on the surface of the unit sphere.

We remark that we can see the poles as two isolated points of the singular representation of the spherical coordinates and where the FP equation has singular coefficients. However, as mentioned below, the PDF is assumed to be regular on the whole domain, therefore we can define the PDF at the poles by continuation. We have

$$\begin{aligned} f_0(t) &:= \lim_{\theta \rightarrow 0^+} f(\varphi, \theta, t) \quad \forall \varphi, \\ f_\pi(t) &:= \lim_{\theta \rightarrow \pi^-} f(\varphi, \theta, t) \quad \forall \varphi. \end{aligned} \quad (3.5)$$

While we are not aware of any analysis on the regularity of solutions of our FP equation, we claim that it is possible to extend results given in Ref. 30 to show the existence of weak solutions to (3.1) in an appropriate θ -weighted Sobolev space and that the solution is Hölder continuous in a neighborhood of the poles. Furthermore, it is possible to use results presented in Ref. 29 to prove the existence of strong solutions to our FP problem.

Now, consider the solution of the FP equation at the poles and focus on structure of this solution as $\theta \rightarrow 0^+$ and $\theta \rightarrow \pi^-$, for all $\varphi \in [0, 2\pi)$. For this purpose, consider (3.1) written in flux form as follows:

$$\partial_t f = \partial_\varphi F^{(1)} + \partial_\theta F^{(2)}, \quad (3.6)$$

with fluxes given by

$$\begin{aligned} F^{(1)}(\varphi, \theta) &= B^{(1)}(\varphi, \theta, u, v)f(\varphi, \theta) + C^{(1)}(\theta)\partial_\varphi f(\varphi, \theta), \\ F^{(2)}(\varphi, \theta) &= B^{(2)}(\varphi, \theta, u, v)f(\varphi, \theta) + C^{(2)}(\theta)\partial_\theta f(\varphi, \theta) \end{aligned} \quad (3.7)$$

and

$$\begin{aligned} B^{(1)}(\varphi, \theta, u, v) &= -\omega - a \cot(\theta)(u \sin(\varphi) + v \cos(\varphi)), \\ C^{(1)}(\theta) &= g \cot^2(\theta/2)/4, \\ B^{(2)}(\varphi, \theta, u, v) &= g(-9 + 2 \cos(\theta) + 3 \cos(2\theta)) \cot(\theta/2)/8 \\ &\quad + a(u \cos(\varphi) - v \sin(\varphi)), \\ C^{(2)}(\theta) &= g \cos^4(\theta/2). \end{aligned} \quad (3.8)$$

By integrating (3.6) on the domain S , we obtain

$$\begin{aligned} \partial_t \int_0^\pi \int_0^{2\pi} f(\varphi, \theta, t) d\varphi d\theta &= \int_0^\pi (F^{(1)}(2\pi, \theta) - F^{(1)}(0, \theta)) d\theta \\ &\quad + \int_0^{2\pi} (F^{(2)}(\varphi, \pi^-) - F^{(2)}(\varphi, 0^+)) d\varphi. \end{aligned}$$

Notice that the left-hand side of this equality is zero due to the conservation of probability. Further, the first integral on the right-hand side is vanishing since we are supposing a regular solution of the FP equation and periodic continuity in φ

must be satisfied. As a result, the solution $f(\varphi, \theta, t)$ of the FP equation is subject to the following condition

$$\int_0^{2\pi} F^{(2)}(\varphi, \pi^-) d\varphi = \int_0^{2\pi} F^{(2)}(\varphi, 0^+) d\varphi. \quad (3.9)$$

According to the flux representation (3.7), we have

$$\begin{aligned} & \int_0^{2\pi} (B^{(2)}(\varphi, \pi^-, u, v) f(\varphi, \pi^-, t) + C^{(2)}(\pi^-) \partial_\theta f(\varphi, \theta, t)|_{\theta=\pi^-}) d\varphi \\ &= \int_0^{2\pi} (B^{(2)}(\varphi, 0^+, u, v) f(\varphi, 0^+, t) + C^{(2)}(0^+) \partial_\theta f(\varphi, \theta, t)|_{\theta=0^+}) d\varphi. \end{aligned} \quad (3.10)$$

The left-hand side of this equation is vanishing, because of $C^{(2)}(\pi^-) = 0$ and $B^{(2)}(\varphi, \pi^-, u, v) = a(u \cos(\varphi) - v \sin(\varphi))$. This follows from the fact that f is supposed to be regular at the pole, see Eq. (3.5), and the integral from 0 to 2π of $\sin(\varphi)$ and $\cos(\varphi)$ are vanishing for all values of the controls (u, v) . As a consequence, the integral on the L.H.S. of (3.10) vanishes.

Further, consider (3.8), with $\theta \rightarrow 0^+$, then $B^{(2)}(\varphi, \theta, u, v) \approx a(u \cos(\varphi) - v \sin(\varphi)) - g/\theta$, that is of order $O(1/\theta)$. This fact and the regularity of f and its derivative, result in

$$f(\varphi, \theta, t) \approx f_{0,1}(\varphi, t)\theta, \quad (3.11)$$

as $\theta \rightarrow 0^+$. This result implies that the R.H.S. of Eq. (3.10) is vanishing. Hence, we obtain the following condition for the PDF on the north pole

$$f_0(t) = \lim_{\theta \rightarrow 0^+} f(\varphi, \theta, t) = 0 \quad \forall \varphi \in [0, 2\pi], \quad t \geq 0. \quad (3.12)$$

On the other hand, we find that on the south pole the PDF can assume values greater than zero.

4. The Fokker–Planck Control Strategy

For the purpose of controlling stochastic processes, in Refs. 12, 17 and 31 probability density function control schemes were proposed, where the objectives depend on the PDF of the stochastic state variable. In this way, deterministic objectives result and no average is needed. In Ref. 17, the objective is defined by the Kullback–Leibler distance between the state PDF and a desired one. On the other hand, in Refs. 12 and 31 a square distance between the state PDF and a desired PDF is considered. Although these works consider deterministic objectives formulated with the PDF, they use stochastic governing models and the state PDF is obtained by averaging or by an interpolation strategy.

We discuss a new approach where PDF objectives are considered in combination with the Fokker–Planck (FP) equation. For one-dimensional stochastic processes, we have investigated this approach in Ref. 1, avoiding all computational difficulties arising in a multidimensional setting. In the present work, we discuss a challenging

multidimensional problem that requires appropriate discretization of the FP optimality system and nonlinear optimization techniques for the resulting nonlinear control problem.

To illustrate our control framework, we consider the control problem formulated in the time window (t_k, t_{k+1}) and assume that the initial value of the process at time t_k is known, in the sense that we give the probability density $\rho(x, s)$ at time $s = t_k$. We formulate the problem to determine a control $(u, v) \in \mathbb{R}^2$ such that starting with initial distribution ρ the process evolves towards a desired target probability density f_d at time $t = t_{k+1}$. This objective can be formulated by the following tracking functional

$$J(f, u, v) := \frac{1}{2} \|f(\cdot, t_{k+1}) - f_d(\cdot, t_{k+1})\|_{L^2(\Omega)}^2 + \frac{\nu}{2}(|u|^2 + |v|^2).$$

Our optimal control problem is formulated as follows. Find $(u, v) \in \mathbb{R}^2$ that minimizes the objective J subject to the constraint given by the Bloch FP equation.

Notice that the solution of the FP model is uniquely determined by the controls and the initial condition; see, e.g. Refs. 16, 26 and 27. We denote this dependence by $f = f(u, v)$ and we assume that the mapping $(u, v) \rightarrow f(u, v)$ is twice differentiable.²¹ Therefore, we can introduce the so-called reduced cost functional \hat{J} given by

$$\hat{J}(u, v) = J(f(u, v), (u, v)). \quad (4.1)$$

In terms of this gradient, a local minimum (u^*, v^*) of the optimal control problem is characterized by $\hat{J}'((u^*, v^*); (\delta u, \delta v)) = 0$ for all $(\delta u, \delta v) \in \mathbb{R}^2$.

For the purpose of characterizing the optimal solution, we define the Lagrangian function

$$\begin{aligned} \mathcal{L}(f, p, u, v) := & J(f, u, v) + \int_{t_k}^{t_{k+1}} \int_0^{2\pi} \int_0^\pi \left\{ \partial_t f + \partial_\varphi (A_\varphi(u, v)f) \right. \\ & + \partial_\theta ((A_\theta(u, v) + a(\theta))f) - \beta(\theta) \partial_\varphi^2 f - \frac{g}{4} \partial_\theta^2 ((1 + \cos(\theta))^2 f) \Big\} \\ & \cdot p(\varphi, \theta, t) d\theta d\varphi dt, \end{aligned}$$

where

$$\alpha(\theta) = g \frac{1 + \cos(\theta)}{\sin(\theta)} \left(1 - \frac{(1 + \cos(\theta)) \cos(\theta)}{4} \right)$$

and

$$\beta(\theta) = \frac{g}{4} \left(\frac{1 + \cos(\theta)}{1 - \cos(\theta)} \right).$$

A cumbersome calculation (see the Appendix), results in the following adjoint FP equation

$$\begin{aligned} -\partial_t p - A_\varphi \partial_\varphi p - \frac{g}{4} \left(\frac{1 + \cos(\theta)}{1 - \cos(\theta)} \right) \partial_\varphi^2 p - \left(A_\theta + g \frac{1 + \cos(\theta)}{\sin(\theta)} \right. \\ \left. \cdot \left(1 - \frac{(1 + \cos(\theta)) \cos(\theta)}{4} \right) \right) \partial_\theta p - \frac{g}{4} (1 + \cos(\theta))^2 \partial_\theta^2 p = 0, \quad (4.2) \end{aligned}$$

with the polar conditions $p(\varphi, 0, t) = 0$ and $p(\varphi, \pi, t) = 0$. This is a parabolic equation marching backwards with starting terminal condition given by

$$p(\varphi, \theta, t_{k+1}) = f_d(\varphi, \theta, t_{k+1}) - f(\varphi, \theta, t_{k+1}). \quad (4.3)$$

Correspondingly, we obtain the following reduced gradient equations that define the optimality conditions for the FP optimal control problem.

$$\begin{aligned} \nabla_u \hat{J}(u, v) &:= \nu u + \int_{t_k}^{t_{k+1}} \int_0^{2\pi} \int_0^\pi \left(\partial_\varphi \left(\frac{\partial A_\varphi}{\partial u} f \right) + \partial_\theta \left(\frac{\partial A_\theta}{\partial u} f \right) \right) p d\theta d\varphi dt = 0, \\ \nabla_v \hat{J}(u, v) &:= \nu v + \int_{t_k}^{t_{k+1}} \int_0^{2\pi} \int_0^\pi \left(\partial_\varphi \left(\frac{\partial A_\varphi}{\partial v} f \right) + \partial_\theta \left(\frac{\partial A_\theta}{\partial v} f \right) \right) p d\theta d\varphi dt = 0, \end{aligned} \quad (4.4)$$

where $p = p(u, v)$ is the solution of the adjoint equation corresponding to $f(u, v)$.

Our purpose is to define a control strategy for the probability density function of a stochastic process to track a given sequence of desired PDFs in time. Let $(0, T)$ be the time interval where the process is considered. We assume time windows of size $\Delta t = T/N$ with N a positive integer. Let $t_k = k\Delta t$, $k = 0, 1, \dots, N$. At time t_0 , we have a given initial PDF denoted with ρ and with $f_d(\cdot, t_k)$, $k = 1, \dots, N$, we denote the sequence of desired PDFs. Our scheme starts at time t_0 and solves the minimization problem $\min_{(u,v)} J(f(u, v), u, v)$ defined in the interval (t_0, t_1) . Then, with the probability density function f resulting at $t = t_1$, that solves the optimal control problem in (t_0, t_1) , we define the initial PDF for the subsequent optimization problem defined in the interval (t_1, t_2) . This procedure is repeated by receding the time horizon until the last time window is reached. This is an instance of the class of receding horizon model predictive control (RH-MPC) schemes^{18,19} that is widely used in engineering applications to design closed-loop algorithms. In fact, we implement an MPC scheme where the time horizon used to evaluate the control coincides with the time horizon where the control is used. One important aspect of this approach is that it can be applied to infinite-dimensional evolution systems,¹⁵ that is the case of the FP model. We refer to Ref. 24 to show that the closed-loop system with the RH-MPC scheme is nominally asymptotically stable.

The RH-MPC procedure is summarized in the following algorithm.

Algorithm 4.1. (RH-MPC Control) Set $k = 0$, $\rho_0 = \rho$:

- (1) Assign the initial PDF, $f(t_k) = \rho_k$ and the target $f_d(\cdot, t_{k+1})$;
- (2) In (t_k, t_{k+1}) , solve $\min_{(u,v) \in \mathbb{R}^2} J(f(u, v), u, v)$ and obtain the optimal control pair (u, v) ;
- (3) If $t_{k+1} < T$, set $k := k + 1$, $\rho_k = f(\cdot, t_k)$, go to 1.
- (4) End.

In Algorithm 4.1, Step (2) consists in solving the optimization problem

$$\min_{(u,v) \in \mathbb{R}^2} \hat{J}(u, v). \quad (4.5)$$

For this purpose, we use a gradient-based scheme, where the gradient components are given by (4.4), that are evaluated as follows.

Algorithm 4.2. (Evaluation of the gradient at (u, v))

- (1) Solve the FP equation (3.1) with given initial condition;
- (2) Solve the adjoint FP equation (4.2) with terminal condition (4.3);
- (3) Compute the gradient components $\nabla_u \hat{J}(u, v)$ and $\nabla_v \hat{J}(u, v)$ given by (4.4) and using numerical quadrature;
- (4) End.

Once the gradient is evaluated, we can solve the optimization problem (4.5) by any gradient-based method; see, e.g. Refs. 6 and 23. We use a nonlinear conjugate gradient (NCG) scheme with Dai–Yuan direction parameter and steplength backtracking search with Armijo condition; see Ref. 6 for all details.

Notice that in our MPC setting, the target f_d is required at the end of all time windows whereas in quantum mechanics it is conceptually difficult to prescribe a desired trajectory. For this purpose, we consider two approaches. In the one case, we take $f_d(\cdot, t_k) = f_d(\cdot)$ for all $k = 1, \dots, N$, that is, we always use the final target at $t = T$. In the other case, we construct a sequence of $f_d(\cdot, t_k)$ obtained by interpolating the initial PDF and the final target at $t = T$. We call the latter setting the tracking case.

5. Discretization of the FP Equation

In this section, we discuss the numerical approximation to our Fokker–Planck equation by using the Chang–Cooper (CC) scheme proposed in Ref. 8. This scheme represents a stable, second-order accurate, positive and conservative numerical scheme for the Fokker–Planck equation. Further, we investigate the discretization of the adjoint FP equation.

To illustrate the CC scheme and discuss its extension to the adjoint equation, consider a sequence of uniform grids $\{S_h\}_{h>0}$ given by

$$S_h = \{(\varphi, \theta) \in \mathbb{R}^2 : \varphi_i = ih_\varphi, \theta_j = jh_\theta, (i, j) \in \mathbb{Z}^2\} \cap S,$$

where $S = (0, \pi) \times [0, 2\pi]$. The mesh sizes h_φ, h_θ are chosen such that the boundaries of S coincide with grid points. We take $h_\theta = \pi/N_\theta$ and $h_\varphi = 2\pi/N_\varphi$.

With ∂_i^- (respectively ∂_i^+) denotes the backward (respectively forward) difference quotient in the i direction, $i = \varphi, \theta$. The second-order derivative in the i direction is given by $\partial_i^2 = \partial_i^- \partial_i^+$.

Let δt be the time step size and N_t denotes the number of time steps. Define

$$Q_{h,\delta t} = \{(\varphi, \theta, t_m) : (\varphi, \theta) \in S_h, t_m = m\delta t, 0 \leq m \leq N_t\}.$$

On this grid, f_{ij}^m denotes the value of a grid function f at φ_i, θ_j and time t_m .

Second-order accuracy in time can be obtained by using a Crank–Nicolson (CN) scheme or by using the following second-order backward differentiation formula (BDF2).

$$\partial_{BD}^- f^m := \frac{3f^m - 4f^{m-1} + f^{m-2}}{2\delta t} \quad \partial_{BD}^+ f^m := -\frac{3f^m - 4f^{m+1} + f^{m+2}}{2\delta t}.$$

In the framework of parabolic optimal control problems, this scheme has been investigated in Ref. 13.

For space discretization, we need a second-order scheme which guarantees positivity of the probability density function together with conservation of the total probability mass. These are essential features that characterize the Chang–Cooper scheme. The first step in the formulation of the CC scheme is to write the FP equation in the conservative flux form (3.6)–(3.7).

Now, consider the FP equation in the following flux form

$$\partial_t f(x, t) = \nabla \cdot F(x, t), \quad (5.1)$$

where $\nabla = (\partial_\varphi, \partial_\theta)$. The conservative discretization of (5.1) is as follows:

$$\frac{1}{\delta t} (f_{i,j}^{m+1} - f_{i,j}^m) = \frac{1}{h_\varphi} (F_{i+1/2,j}^{(1)} - F_{i-1/2,j}^{(1)}) + \frac{1}{h_\theta} (F_{i,j+1/2}^{(2)} - F_{i,j-1/2}^{(2)}). \quad (5.2)$$

The flux in the φ th-direction is given by

$$\begin{aligned} F_{i+1/2,j}^{(1)} = & \left[(1 - \delta_{i,j}^{(1)}) B_{i+1/2,j}^{(1)} + \frac{1}{h} C_{i+1/2,j}^{(1)} \right] f_{i+1/2,j}^{m+1} \\ & - \left(\frac{1}{h} C_{i+1/2,j}^{(1)} - \delta_{i,j}^{(1)} B_{i+1/2,j}^{(1)} \right) f_{i,j}^{m+1}, \end{aligned} \quad (5.3)$$

where the coefficients B, C are estimated at the time level m .

This formula results from the following linear convex combination of f^{m+1} at the points i, j and $i+1, j$. We have

$$f_{i+1/2,j}^{m+1} = (1 - \delta_{i,j}^{(1)}) f_{i+1,j}^{m+1} + \delta_{i,j}^{(1)} f_{i,j}^{m+1}, \quad \delta_{i,j}^{(1)} \in [0, 1/2].$$

In the θ direction, we have a similar formula

$$f_{i,j+1/2}^{m+1} = (1 - \delta_{i,j}^{(2)}) f_{i,j+1}^{m+1} + \delta_{i,j}^{(2)} f_{i,j}^{m+1}, \quad \delta_{i,j}^{(2)} \in [0, 1/2].$$

In Ref. 8 it is shown that the parameter $\delta_{i,j}^{(k)}$, $k = 1, 2$, can be chosen such that the resulting scheme preserves equilibrium configurations, is conservative and guarantees positivity of the solution. This choice is as follows:

$$\delta_{i,j}^{(k)} = \frac{1}{w_{i,j}^{(k)}} - \frac{1}{\exp(w_{i,j}^{(k)}) - 1}, \quad k = 1, 2,$$

where $w_{i,j}^{(1)} = h B_{i+1/2,j}^{(1)} / C_{i+1/2,j}^{(1)}$ and $w_{i,j}^{(2)} = h B_{i,j+1/2}^{(2)} / C_{i,j+1/2}^{(2)}$.

Next, we discuss the discretization of the adjoint equation. Notice that the discretization of the forward- and adjoint FP equations influences the accuracy of the

reduced gradient used in our optimization scheme; see Ref. 7 for a detailed discussion in the case of control of flows. In fact, a numerically correct gradient, in the sense that it is consistent with the objective defined by quadratures, is obtained when the discretization scheme of the adjoint equation is the algebraic adjoint of the scheme used for the forward problem. Concerning the time derivative, we need to formally replace the backward scheme with the forward scheme. Less straightforward is to determine the discretization scheme corresponding to the adjoint spatial discretization because of the presence of first- and second-order differential operators. However, by writing the FP equation in flux form and because the divergence of the flux is evaluated by centered schemes, the adjoint equation should have a spatial stencil which corresponds to the transpose of the forward stencil. It is interesting to obtain this result directly by deriving the adjoint equation from the discrete Lagrangian and performing discrete integration by parts.

To illustrate this procedure, we consider an example in a one-dimensional space. (Therefore we drop the index k in $\delta^{(k)}$.) Using simple quadratures, the discrete version of the integral term $\int (\nabla F) pdx$ becomes

$$\sum_i (F_{i+1/2} - F_{i-1/2}) p_i. \quad (5.4)$$

We write (5.3) as follows:

$$F_{i+1/2} = K_{i+1/2} f_{i+1}^{m+1} - R_{i+1/2} f_i^{m+1}, \quad (5.5)$$

where

$$\begin{cases} K_{i+1/2} = (1 - \delta_i) B_{i+1/2} + \frac{1}{h} C_{i+1/2}, \\ R_{i+1/2} = \frac{1}{h} C_{i+1/2} - \delta_i B_{i+1/2}. \end{cases} \quad (5.6)$$

Using these definitions in (5.4) we have

$$\sum_i [(K_{i+1/2} f_{i+1}^{m+1} - R_{i+1/2} f_i^{m+1}) - (K_{i-1/2} f_i^{m+1} - R_{i-1/2} f_{i-1}^{m+1})] p_i. \quad (5.7)$$

Next, we recast the summation to collect the terms f_i with the same space index. We have

$$\begin{aligned} \sum_{i=0}^I K_{i+1/2} f_{i+1}^{m+1} p_i &\rightarrow \sum_{i=1}^{I+1} K_{i-1/2} f_i^{m+1} p_{i-1}, \\ \sum_{i=0}^I R_{i-1/2} f_{i-1}^{m+1} p_i &\rightarrow \sum_{i=-1}^{I-1} R_{i+1/2} f_i^{m+1} p_{i+1}. \end{aligned}$$

Therefore, we obtain

$$\sum_i (K_{i-1/2} p_{i-1} - R_{i+1/2} p_i - K_{i-1/2} p_i + R_{i+1/2} p_{i+1}) f_i^{m+1}.$$

Now, we consider the variation with respect to f_i^{m+1} including also the time-derivative term. We obtain the following discrete adjoint equation:

$$-\frac{1}{\delta t}(p_i^{m+1} - p_i^m) = \frac{1}{h}[(K_{i-1/2}p_{i-1}^m - R_{i+1/2}p_i^m) \\ - (K_{i-1/2}p_i^m + R_{i+1/2}p_{i+1}^m)], \quad (5.8)$$

which represents a backward evolution equation with implicit discretization. A comparison, with (5.2) and (5.3) shows that the adjoint equation is the transpose of the forward state equation.

At the time step m , the solution of the FP equation corresponds to solving a system of the form $Hf^{m+1} = b(f^m, f^{m-1})$, where the matrix of coefficients H is built from the Chang–Cooper method and the BDF2 time step formula. In our algorithm the unknown f is arranged in a vector composed of block of vectors, each block contains the values with constant latitude θ , that is,

$$f = (f_0, \dots, f_0, f_{1,1}, \dots, f_{N_\varphi,1}, \dots, f_{1,N_\theta}, \dots, f_{N_\varphi,N_\theta}, f_\pi, \dots, f_\pi).$$

The first and the last vector blocks (f_0, \dots, f_0) and (f_π, \dots, f_π) represent the discrete function at the north and south poles, respectively. The value on the pole is repeated N_φ times for convenience of representation.

For the adjoint problem, we solve $H'p^m = b'(p^{m+1}, p^{m+2})$ at each time step in a backward sequence. Here, H' is obtained from H taking the transpose and setting to zero all the first and the last rows and columns of the matrix H , that are related to the poles.

We obtain the values at the poles as follows. Let us define the average probabilities in balls with radius $\epsilon > 0$ centered at the south and north poles, respectively. We have

$$f_{0,\epsilon}(t) := \frac{1}{2\pi\epsilon} \int_0^\epsilon \int_0^{2\pi} f(\varphi, \theta, t) d\theta d\varphi \quad (5.9)$$

and

$$f_{\pi,\epsilon}(t) := \frac{1}{2\pi\epsilon} \int_{\pi-\epsilon}^\pi \int_0^{2\pi} f(\varphi, \theta, t) d\theta d\varphi, \quad (5.10)$$

so that $\lim_{\epsilon \rightarrow 0^+} f_{0,\epsilon}(t) = f_0(t)$ and $\lim_{\epsilon \rightarrow 0^+} f_{\pi,\epsilon}(t) = f_\pi(t)$, as defined in (3.5), that is consistent with the continuous model. Furthermore, by using an analysis based on the fluxes similar to that performed with (3.6), it is possible to show that the functions defined in (5.9) and (5.10) satisfy the following equations

$$\frac{d}{dt} f_{0,\epsilon}(t) = \frac{1}{2\pi\epsilon} \int_0^{2\pi} F^{(2)}(\varphi, \epsilon, t) d\varphi \quad (5.11)$$

and

$$\frac{d}{dt} f_{\pi,\epsilon}(t) = \frac{-1}{2\pi\epsilon} \int_0^{2\pi} F^{(2)}(\varphi, \pi - \epsilon, t) d\varphi. \quad (5.12)$$

Finally, to obtain the values of the PDF at the poles, we implement the following implicit scheme. At the south pole, we have

$$f_{\pi}^{m+1} + \delta t \frac{h_{\varphi}}{\pi h_{\theta}} \sum_i F_{i,\pi-1/2}^{(2)} = f_{\pi}^m, \quad (5.13)$$

where f_{π}^{m+1} enters in the evaluation of the fluxes $F_{i,\pi-1/2}^{(2)}$. At the north pole, we have

$$f_0^{m+1} - \delta t \frac{h_{\varphi}}{\pi h_{\theta}} \sum_i F_{i,0+1/2}^{(2)} = f_0^m, \quad (5.14)$$

where f_0^{m+1} enters in the evaluation of the fluxes $F_{i,0+1/2}^{(2)}$. Notice that the formulation (5.13) and (5.14), uses the setting of (5.11) and (5.12) with $\epsilon = h_{\theta}/2$. We remark that, according to (3.12), the computed f_0^m tends to zero as the mesh is refined.

The effort to define the evolution equations (5.11) and (5.12) and correspondingly the discrete equations (5.13) and (5.14), is motivated also by the requirement that these equations result in a meaningful adjoint system in both the continuous and the discrete frameworks. We remark that these equations result from consideration of regularity and conservativeness of the forward problem and the intrinsic singularity of the coordinate system. Therefore these conditions are formulated in addition to the FP equation and hence they do not have an immediate adjoint counterpart. On the other hand, based on regularity requirements we obtain conditions for the adjoint variable on the poles.

To estimate the gradients using (4.4), we use a simple quadrature formula that is given below for computing the discrete L^2 -norm.

$$\|f\|^2 = h_{\varphi} h_{\theta} \sum_{i=1}^{N_{\varphi}} \sum_{j=1}^{N_{\theta}} f_{i,j}^2 + \pi h_{\theta} (f_0^2 + f_{\pi}^2).$$

6. Numerical Experiments

In this section, we show results of numerical experiments for the optimal control of the PDF of the spin orientation of a two-level system. Parameters of the model are $g = 1$, $\omega = 0.01$, $a = 7g/\sqrt{2}$, corresponding to the heterodyne detection device setting of Ref. 32. The initial position of the spin is supposed to be known with an indeterminacy in the position described by a bivariate Gauss density distribution on the Bloch sphere. We set a Gaussian distribution on the tangent plane to the sphere at the average position of the spin, then we make a projection on the sphere surface. Two test cases of spin orientation are considered in the following. In the first case, the spin orientation starts at the equator and driven towards the south pole. In the other case, the spin starts at the south pole and is required to reach the equator. These tests allow us to simulate the real case of control of the total magnetization orientation with respect to an external magnetic field, in order to

perform some useful task, like energy level transition for memory devices or electromagnetic emission for spectroscopy purposes. According to the previous discussion, we consider two MPC control strategies with and without target tracking.

In the first experiment, we set the initial PDF as Gaussian placed at the equator with variances value equal to $\sigma = \pi/20$ in both directions, see the left of Fig. 2. A Gaussian target is placed at the south pole, with variance $\sigma = \pi/8$. The optimization problem is performed over $N = 10$ time windows, up to the final time $T = 4$. The aim of the control is to drive the PDF towards the south pole. We choose a grid of $N_\theta \times N_\varphi$ points, where $N_\theta = 30$ and $N_\varphi = 60$, and a time step size $\delta t = 4/300$. We choose $\nu = 10^{-3}$ unless otherwise specified. The final distribution is shown on the right of Fig. 2.

In Table 1, we report the maximum norm of the difference between the given final target and the controlled PDF, $\|f(\cdot, t_{k+1}) - f_d(\cdot)\|_\infty$. In the third and fourth columns, we report the values of control values u and v . We see that the norm of the difference decreases as the time elapses, according to the aim of the optimization process. In Fig. 2, the initial PDF and the resulting final PDF at the south pole are depicted.

In the next experiment, we show results of a numerical test with the use of the tracking strategy. The initial PDF condition ρ is a narrow normalized bi-dimensional Gaussian placed at the equator at $(\theta, \phi) = (\pi/2, \pi)$ with variances equal to $\sigma = \pi/20$ (see Fig. 3). The aim is to reach a final desired Gaussian PDF target at the south pole with variances $\sigma = \pi/8$. The tracking is achieved by moving the desired target from the initial position to the final one, with constant speed

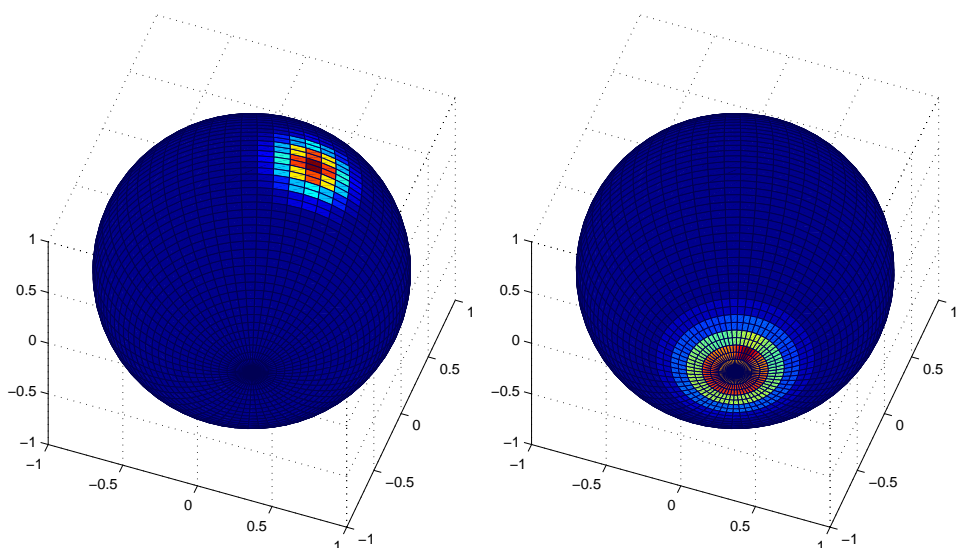


Fig. 2. Control on the Bloch sphere: The initial PDF on the equator (left) and the final PDF configuration at the south pole resulting from action of the optimal control.

Table 1. Results for equator-to-south pole control.

Space mesh $N_\theta \times N_\varphi = 30 \times 60$, time mesh $N_t = 30$			
Time	$\ f(t_k) - f_d(t_k)\ $	u	v
0.0	6.82130	0.00000	0.00000
0.4	0.33293	-2.38191	-0.00050
0.8	0.30834	0.05045	-0.00079
1.2	0.29090	-0.03406	0.00060
1.6	0.26529	0.00688	-0.00007
2.0	0.23175	0.00041	-0.00001
2.4	0.18452	-0.00012	0.00000
2.8	0.18064	-0.00001	0.00000
3.2	0.25446	-0.00014	0.00001
3.6	0.33804	-0.00014	0.00001
4.0	0.40457	-0.00014	0.00001

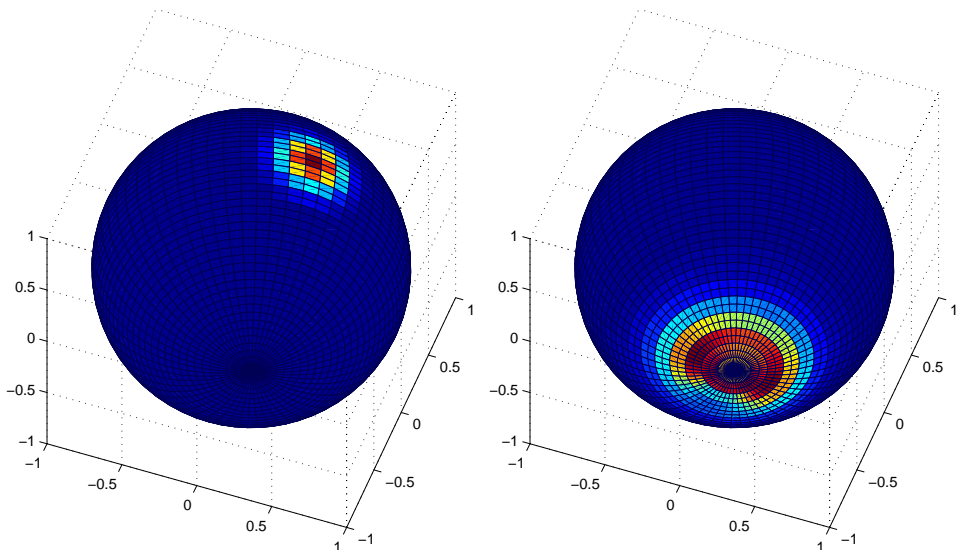


Fig. 3. Control on the Bloch sphere: The initial PDF on the equator (left) and the final PDF configuration at the south pole resulting from action of the optimal control with tracking function.

along the longitudinal geodetic and with linearly increasing variances according to the law $\sigma(t_k) = \pi/20 + t_k(\pi/8 - \pi/20)/T$.

We consider a time horizon of $T = 4$ and $N = 10$ time windows. Discretization grid is with $N_\theta = 30$ and $N_\varphi = 60$, and a time step size $\delta t = 4/300$. In Fig. 4, we plot the maximum norm of the difference between the time-varying target and the controlled PDF, $\|f(\cdot, t_{k+1}) - f_d(\cdot, t_{k+1})\|_\infty$. We see that the norm of the tracking error decreases as the time elapses, according to the purpose of the control. Results for this experiment are reported in Table 2. These results are less sensitive to the choice of the weight ν . On the other hand, similar controls are obtained using finer meshes as shown in Table 3.

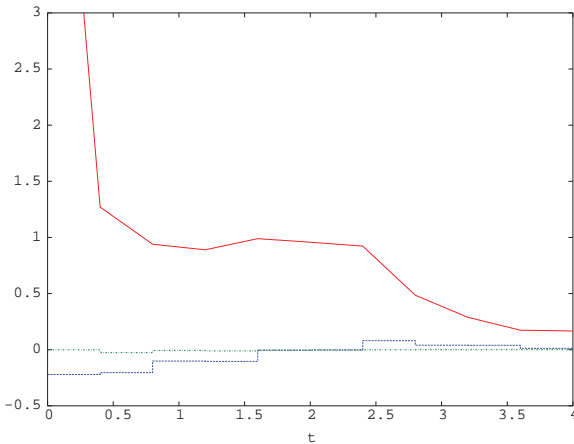


Fig. 4. Control on the Bloch sphere: The target error $\|f(\cdot, t_k) - f_d(\cdot, t_{k+1})\|_\infty$ (continuous line) and the controls (u, v) in $(0, T)$.

Table 2. Results for equator-to-south pole with target tracking.

Space mesh $N_\theta \times N_\varphi = 30 \times 60$, time mesh $N_t = 30$			
Time	$\ f(t_k) - f_d(t_k)\ $	u	v
0.0	6.82130	0.00000	0.00000
0.4	1.27019	-0.22099	-0.00168
0.8	0.93939	-0.20444	-0.02627
1.2	0.89002	-0.10130	-0.00627
1.6	0.98887	-0.10448	-0.01121
2.0	0.95728	-0.00528	-0.00341
2.4	0.92259	-0.00377	-0.00011
2.8	0.48519	0.08002	-0.00113
3.2	0.28848	0.04005	-0.00049
3.6	0.17412	0.03896	-0.00012
4.0	0.16638	0.01185	-0.00004

Table 3. Results for equator-to-south pole control with target tracking and finer mesh.

Space mesh $N_\theta \times N_\varphi = 60 \times 120$, time mesh $N_t = 60$			
Time	$\ f(t_k) - f_d(t_k)\ $	u	v
0	6.8291	0	0
0.4	1.12104	-0.21060	-0.00056
0.8	0.87337	-0.18612	-0.02753
1.2	0.85286	-0.13002	-0.01884
1.6	0.92772	-0.08333	-0.01179
2.0	1.03689	-0.03702	-0.00358
2.4	0.95766	0.02342	-0.00941
2.8	0.62508	0.06238	0.00745
3.2	0.30070	0.06044	-0.00230
3.6	0.26495	0.02922	-0.00000
4.0	0.32530	0.01656	-0.00016

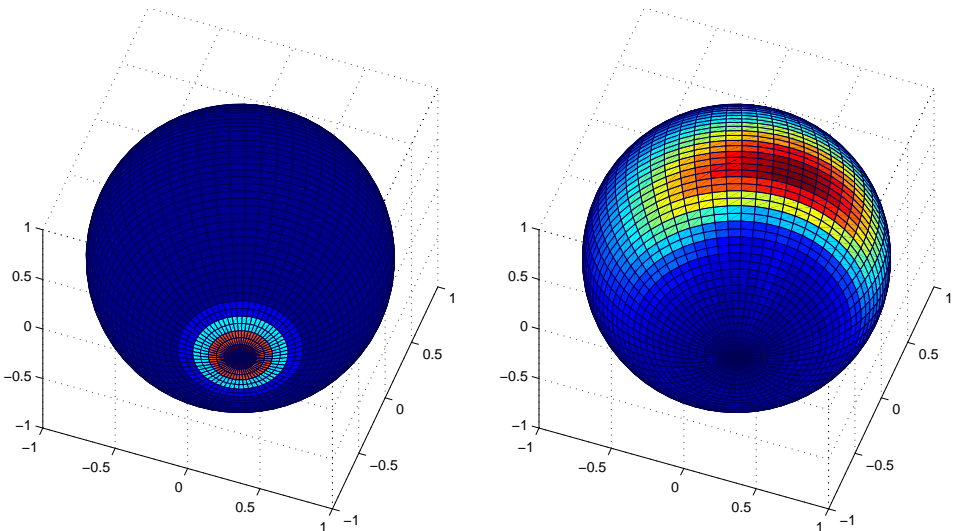


Fig. 5. Control on the Bloch sphere: The initial PDF (left) at the south pole and the final PDF configuration on the equator resulting from the action of the optimal control.

In the following experiment, we deal with the problem of driving the spin from the south pole to a point on the equator. For this case, we depict in Fig. 5 the action of the control on the Bloch sphere considering a time horizon of $T = 10$ and $N = 20$ time windows. The desired target configuration moves from the south pole to the equator with a law similar to that of the previous test.

The values for the maximum norm of the difference between the given target and the controlled PDF, $\|f(\cdot, t_{k+1}) - f_d(\cdot, t_{k+1})\|_\infty$ and the control values are shown in Table 4, where we report the norm of the tracking error corresponding to every second time window. Also in this case, we see that the norm difference decreases as the time elapses, aside for the last time window.

Table 4. Results for south-pole-to-equator control with target tracking.

Space mesh $N_\theta \times N_\varphi = 30 \times 60$, time mesh $N_t = 30$			
Time	$\ f(t_k) - f_d(t_k)\ $	u	v
0.0	1.36159	0.00000	0.00000
1.0	1.36159	0.00000	-0.00000
2.0	1.40788	0.00000	-0.00000
3.0	1.45394	0.03152	-0.00111
4.0	1.36159	0.05083	-0.00363
5.0	2.97961	-0.01794	-0.00561
6.0	2.43220	-0.19092	-0.00104
7.0	1.44380	-0.19873	-0.00371
8.0	0.92509	-0.25891	-0.02059
9.0	0.92553	-0.29983	-0.26907
10.0	0.99224	-0.32036	-0.00287

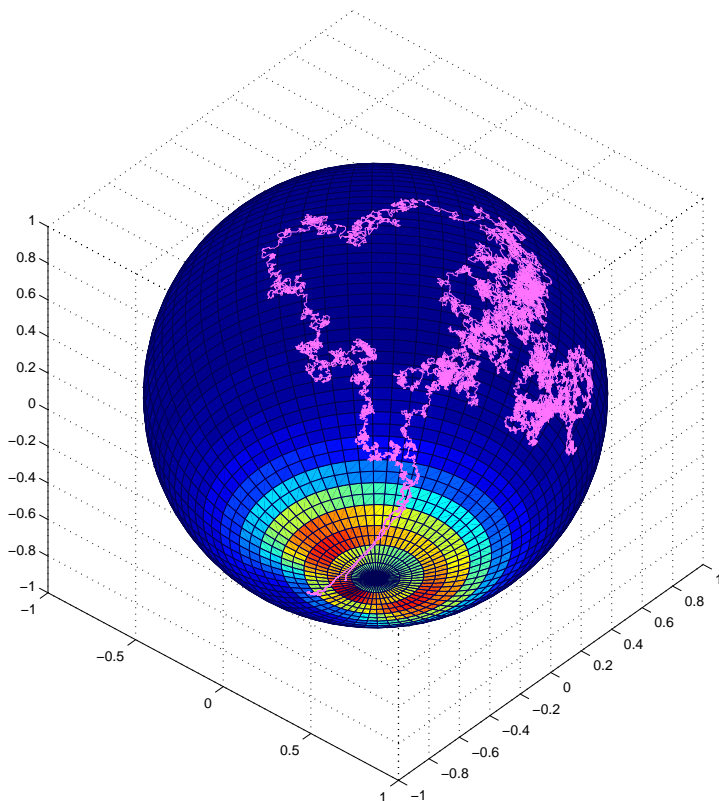


Fig. 6. Two controlled stochastic trajectories starting at the equator and reaching the south pole.

In Fig. 6, we plot two stochastic trajectories on the Bloch sphere. These trajectories correspond to the first experiment with tracking, where an optimal control is sought to drive the spin from the equator to the south pole orientation. The resulting optimal control is plugged in the stochastic model (2.9) that is approximated using the Euler–Maruyama scheme; see, e.g. Ref. 14.

7. Conclusion

Motivated by the need to develop robust control strategies for nano-devices, a representative two-level open quantum system subject to dissipation due to environment losses and stochastic perturbation was considered. The evolution of this system is governed by a Lindblad master equation which is augmented by a stochastic term to model the effect of time-continuous measurements.

The aim of this work was to define a framework for the design of robust controls that are able to drive the probability density of the configurations of the quantum system. For this purpose a Fokker–Planck control framework was proposed, where the control objectives are defined based on the probability density functions of the

two-level stochastic process and the controls are computed as minimizers of these objectives subject to the constraints represented by the Fokker–Planck equation. In particular, a detailed analysis for the formulation of the adjoint problem was presented. The implementation of the resulting open-loop controls was realized with a receding-horizon algorithm over a sequence of time windows. Results of numerical experiments demonstrated the effectiveness of the proposed approach.

Appendix A. The Adjoint Equation

Consider the Lagrange function corresponding to our FP control problem defined in the time interval $(0, T)$. We have

$$\begin{aligned} \mathcal{L}(f, p, u, v) := & J(f, u, v) + \int_0^T \int_0^{2\pi} \int_0^\pi \left\{ \partial_t f + \partial_\varphi (A_\varphi f) \right. \\ & + \partial_\theta ((A_\theta + \alpha(\theta))f) - \beta(\theta) \partial_\varphi^2 f - \frac{g}{4} \partial_\theta^2 ((1 + \cos(\theta))^2 f) \Big\} \\ & \cdot p(\varphi, \theta, t) d\theta d\varphi dt. \end{aligned} \quad (\text{A.1})$$

The adjoint FP equation characterizes the extremal points of \mathcal{L} with respect to variations of the state f . That is, it represents the gradient equation $(\nabla_f \mathcal{L}(f, p, u), \delta f) = 0$ for all variations δf in an appropriate functional space. In order to guarantee a well-defined Lagrange function and also the applicability of the Fubini's theorem for the calculation that follows, the integral in (A.1) is required to be convergent. We are assuming that f and its derivatives are enough regular so that $\partial_t f$ is integrable. The second term inside the integral contains A_φ that is singular for $\theta = 0$ and $\theta = \pi$ due to $\cot(\theta)$. Since $f_0(t) = 0$, i.e. condition (3.12), the singularity in $\theta = 0$ is removed. In $\theta = \pi$ there are no constraints to f , hence we have

$$\lim_{\theta \rightarrow \pi^-} p(\varphi, \theta, t) = 0, \quad (\text{A.2})$$

that is,

$$p(\varphi, \theta, t)|_{\theta \simeq \pi^-} \simeq p_{\pi, 1}(\varphi, t)(\pi - \theta). \quad (\text{A.3})$$

The singularity in $\alpha(\theta)$ for $\theta = 0$ of the third term is erased from (3.12). The fourth term contains $\beta(\theta)$ that diverges as $1/\theta^2$ as $\theta \simeq 0$, so that in order to regularize it, the condition $f_0(t) = 0$ is not sufficient and the following

$$\lim_{\theta \rightarrow 0^+} p(\varphi, \theta, t) = 0 \quad (\text{A.4})$$

has to be included.

The conditions of (A.4) and (A.2) are fundamental for the correct definition of the Lagrange function.

Now we can proceed to do variation of the Lagrange function and using integration by part, we obtain the adjoint equation.

From our discussion on the properties of the solution of the Fokker–Planck equation close to the north pole, we obtain (3.12), therefore also $\lim_{\theta \rightarrow 0^+} \delta f(\varphi, \theta, t) = 0$.

For this reason, as $\theta \rightarrow 0^+$ we assume the expansion

$$\delta f(\varphi, \theta, t) \simeq \delta f_{0,1}(\varphi, t)\theta. \quad (\text{A.5})$$

Now, we analyze the variations term-by-term in the Lagrange function. Concerning the time derivative term, we have

$$\int_0^T \int_0^{2\pi} \int_0^\pi \partial_t \delta f p = \int_0^\pi \int_0^{2\pi} [p \delta f]_0^T - \int_0^T \int_0^{2\pi} \int_0^\pi \delta f \partial_t p,$$

where the first integral enters in the construction of the final condition for the adjoint equation. In fact, including the result of the variation of f in J , we obtain the following

$$p(\varphi, \theta, T) + f(\varphi, \theta, T) - f_d(\varphi, \theta) = 0. \quad (\text{A.6})$$

Next, consider the second term

$$\int_0^T \int_0^\pi [p A_\varphi \delta f]_0^{2\pi} d\theta dt - \int_0^T \int_0^{2\pi} \int_0^\pi (A_\varphi \delta f) \partial_\varphi p d\theta d\varphi dt.$$

Notice that in the boundary integral we can exchange the order of integration thanks to Fubini's theorem. This integrand function is zero for the periodic continuity in φ of the involved functions.

Now, consider the third term in the Lagrange function. We have

$$\int_0^T \int_0^{2\pi} [(A_\theta + \alpha(\theta)) \delta f p]_{0+}^\pi d\varphi dt - \int_0^T \int_0^{2\pi} \int_0^\pi (A_\theta + \alpha(\theta)) \delta f \partial_\theta p d\theta d\varphi dt.$$

We note that in the first integral we have $A_\theta + \alpha(\theta)|_{\theta \approx 0} \approx -a(u \cos(\varphi) - v \sin(\varphi)) + g/\theta$. The singularity in $\theta = 0$ is removed from (A.5) and the integral vanishes because (A.4) holds. Hence,

$$\int_0^T \int_0^{2\pi} \lim_{\theta \rightarrow 0} (-a(u \cos(\varphi) - v \sin(\varphi)) + g/\theta) \delta f_{0,1}(\varphi, t) \theta p d\varphi dt = 0.$$

For $\theta \simeq \pi$ the following integral

$$\int_0^T \int_0^{2\pi} \lim_{\theta \rightarrow \pi} (-a(u \sin(\varphi) + v \cos(\varphi))) \delta f_\pi(t) p(\varphi, \theta, t) d\varphi dt$$

vanishes because of the condition (A.2).

The fourth term in the Lagrangian contains the second derivatives in φ . We have

$$\begin{aligned} & - \int_0^T \int_0^\pi \beta(\theta) [p \partial_\varphi \delta f]_0^{2\pi} d\theta dt + \int_0^T \int_0^\pi \beta(\theta) [\delta f \partial_\varphi p]_0^{2\pi} d\theta dt \\ & - \int_0^T \int_0^{2\pi} \int_0^\pi \beta(\theta) \delta f \partial_\varphi^2 p d\theta d\varphi dt. \end{aligned}$$

Here, $\beta(\theta)$ diverges as g/θ^2 as θ approaches to zero, but it is regularized from both (3.12) and (A.4), then as above Fubini's theorem is applicable. Therefore the integrand functions are zero for the continuous periodic condition in φ .

Finally, we consider the last term in the Lagrange function

$$\begin{aligned} & -\frac{g}{4} \int_0^T \int_0^{2\pi} [p \partial_\theta ((1 + \cos(\theta))^2 \delta f)]_0^\pi d\varphi dt - \frac{g}{4} \int_0^T \int_0^{2\pi} [((1 + \cos(\theta))^2 \delta f) \partial_\theta p]_0^\pi d\varphi dt \\ & - \frac{g}{4} \int_0^T \int_0^{2\pi} \int_0^\pi ((1 + \cos(\theta))^2 \delta f) \partial_\theta^2 p d\theta d\varphi dt, \end{aligned}$$

where there are no singularities. The first integrand function evaluated at $\theta = \pi$ and at $\theta = 0$ is zero because of (A.4) and (A.2). The second boundary integral is zero in $\theta = 0$ because of (A.5) and in $\theta = \pi$ since the term $1 + \cos(\theta)$ vanishes.

Summarizing, we obtain the following adjoint FP equation

$$\begin{aligned} & -\partial_t p - A_\varphi \partial_\varphi p - \frac{g}{4} \left(\frac{1 + \cos(\theta)}{1 - \cos(\theta)} \right) \partial_\varphi^2 p - \left(A_\theta + g \frac{1 + \cos(\theta)}{\sin(\theta)} \right. \\ & \cdot \left. \left(1 - \frac{(1 + \cos(\theta)) \cos(\theta)}{4} \right) \right) \partial_\theta p - \frac{g}{4} (1 + \cos(\theta))^2 \partial_\theta^2 p = 0, \quad (\text{A.7}) \end{aligned}$$

with the boundary conditions $p_0(t) = p(\varphi, 0^+, t) = 0$, $p_\pi(t) = p(\varphi, \pi^-, t) = 0$ and terminal condition

$$p(\varphi, \theta, T) = -(f(\varphi, \theta, T) - f_d(\varphi, \theta)).$$

Acknowledgment

This work was supported in part by DFG Project “Controllability and Optimal Control of Interacting Quantum Dynamical Systems” and European Science Foundation ESF OPTPDE Programme Grant.

References

1. M. Annunziato and A. Borzì, Optimal control of probability density functions of stochastic processes, *Math. Model. Anal.* **15** (2010) 393–407.
2. A. Barchielli and M. Gregoratti, *Quantum Trajectories and Measurements in Continuous Time* (Springer, 2009).
3. K. Beauchard, J.-M. Coron and P. Rouchon, Controllability issues for continuous-spectrum systems and ensemble controllability of Bloch equations, *Commun. Math. Phys.* **296** (2010) 525–557.
4. B. Bonnard and D. Sugny, Time-minimal control of dissipative two-level quantum systems: The integrable case, *SIAM J. Control Optim.* **48** (2009) 1289–1308.
5. A. Borzì, J. Salomon and S. Volkwein, Formulation and numerical solution of finite-level quantum optimal control problems, *J. Comput. Appl. Math.* **216** (2008) 170–197.
6. A. Borzì and V. Schulz, *Computational Optimization of Systems Governed by Partial Differential Equations* (SIAM, 2012).
7. J. Burkardt, M. Gunzburger and J. Peterson, Insensitive functionals, inconsistent gradients, spurious minima, and regularized functionals in flow optimization problems, *Int. J. Comput. Fluid Dynam.* **16** (2002) 171–185.
8. J. S. Chang and G. Cooper, A practical scheme for Fokker–Planck equations, *J. Comput. Phys.* **6** (1970) 1–16.

9. E. B. Davies, *Quantum Theory of Open Systems* (Academic Press, 1976).
10. G. Dirr, U. Helmke, I. Kurniawan and T. Schulte-Herbrüggen, Lie-semigroup structures for reachability and control of open quantum systems: Kossakowski–Lindblad generators from Lie wedge to Markovian channels, *Rep. Math. Phys.* **64** (2009) 93–121.
11. N. Gisin and I. C. Percival, The quantum-state diffusion model applied to open systems, *J. Phys. A: Math. Gen.* **25** (1992) 56–77.
12. M. G. Forbes, M. Guay and J. F. Forbes, Control design for first-order processes: Shaping the probability density of the process state, *J. Process Control* **14** (2004) 399–410.
13. S. González Andrade and A. Borzì, Multigrid second-order accurate solution of parabolic control-constrained problems, *Comput. Optim. Appl.* **51** (2012) 835–866.
14. D. J. Higham, An algorithmic introduction to numerical simulation of stochastic differential equations, *SIAM Rev.* **43** (2001) 525–546.
15. K. Ito and K. Kunisch, Receding horizon optimal control for infinite-dimensional systems, *ESAIM: Control, Optim. Cal. Var.* **35** (1990) 814–824.
16. R. Jordan, D. Kinderlehrer and F. Otto, Variational formulation of the Fokker–Planck equation, *SIAM J. Math. Anal.* **29** (1998) 1–17.
17. G. Jumarie, Tracking control of nonlinear stochastic systems by using path cross-entropy and Fokker–Planck equation, *Int. J. Syst. Sci.* **23** (1992) 1101–1114.
18. D. Q. Mayne and H. Michalska, Receding horizon control for nonlinear systems, *IEEE Trans. Aut. Control* **35** (1990) 814–824.
19. L. Magni, D. M. Raimondo and F. Allgöwer, *Nonlinear Model Predictive Control* (Springer, 2009).
20. H. Lan and Y. Ding, Ordering, positioning and uniformity of quantum dot arrays, *Nanotoday* **7** (2012) 94–123.
21. J. L. Lions, *Optimal Control of Systems Governed by Partial Differential Equations* (Springer, 1971).
22. Y. Maday, J. Salomon and G. Turinici, Monotonic time-discretized schemes in quantum control, *Numer. Math.* **103** (2006) 323–338.
23. J. Nocedal and S. J. Wright, *Numerical Optimization* (Springer, 1999).
24. Y. Ou and E. Schuster, On the stability of receding horizon control of bilinear parabolic PDE systems, *Proc. of the 2010 IEEE Conference on Decision and Control*, Atlanta, Georgia, December 15–17, 2010.
25. C. Pellegrini, Existence, uniqueness and approximation of a stochastic Schrödinger equation: The diffusive case, *Ann. Probab.* **36** (2008) 2332–2353.
26. S. Primak, V. Kontorovich and V. Lyandres, *Stochastic Methods and Their Applications to Communications* (John Wiley and Sons, 2004).
27. R. Risken, *The Fokker–Planck Equation: Methods of Solution and Applications* (Springer, 1996).
28. R. Roloff, M. Wenin and W. Pötz, Optimal control for open quantum systems: Qubits and quantum gates, *J. Comput. Theor. Nanosci.* **6** (2009) 1837–1863.
29. M. Schechter, On the Dirichlet problem for second order elliptic equations with coefficients singular at the boundary, *Commun. Pure Appl. Math.* **13** (1960) 321–328.
30. P. D. Smith, A regularity theorem for a singular elliptic equation, *Appl. Anal.* **14** (1983) 223–236.
31. H. Wang, Robust control of the output probability density functions for multivariable stochastic systems with guaranteed stability, *IEEE Trans. Aut. Control* **44** (1999) 2103–2107.
32. H. M. Wiseman and G. J. Milburn, Interpretation of quantum jump and diffusion processes illustrated on the Bloch sphere, *Phys. Rev. A* **47** (1993) 1652–1666.